

Diffractive Production of $b\bar{b}$ in Proton - Antiproton Collision at the Tevatron

GILVAN ALVES^{a)*}, EUGENE LEVIN^{b)c)†}
and
ALBERTO SANTORO^{a)c)*}

^{a)}*LAFEX, Centro Brasileiro de Pesquisas Físicas (CNPq)
Rua Dr. Xavier Sigaud 150, 22290 - 180 Rio de Janeiro, RJ, BRAZIL*

^{b)}*Theory Department, Petersburg Nuclear Physics Institute
188350, Gatchina, St. Petersburg, RUSSIA*

^{c)}*Fermi National Accelerator Laboratory
P.O. 500 Batavia Illinois -60510 U.S.A.*

Abstract: We show that the cross section of the diffractive production of $b\bar{b}$ can be described as the sum of two contributions: the first is proportional to the probability of finding a small size $b\bar{b}$ color dipole in the fast hadron wave function before the interaction with a target, while the second is the $b\bar{b}$ -production after or during the interaction with the target. The formulae are presented as well as the discussion of the interrelation between these two contributions and the Ingelman -Schlein and coherent diffraction mechanisms. The main prediction is that the coherent diffraction mechanism dominates, at least at the Tevatron energies, giving the unique possibility to study it experimentally.

* E-mail: gilvan@lafex.cbpf.br

† E-mail: levin@fnal.gov; leving@ccsg.tau.ac.il

* E-mail: santoro@fnal.gov;santoro@lafex.cbpf.br

1 Introduction.

The main goal of this letter is to consider the possibility of measuring the inelastic cross section in the diffractive kinematic region and to discuss the diffractive production of $b\bar{b}$ - pair as a way to extract the value of gluon structure function ($x_{Bj}G(x_{Bj}, Q^2)$) in the region of small x_{Bj} . New HERA data [1] shows a rapid increase of $F_2(x_{Bj}, Q^2)$ in the region of small x_{Bj} ($x_{Bj} < 10^{-2}$), which could be interpreted as a manifestation of the growth of the gluon structure function at small x_{Bj} . However, the data on F_2 does not allow the extraction of the value of the gluon structure function within good accuracy. At the present we know the gluon structure function with accuracy up to factor two (see Fig. 1, that shows the gluon structure in three parametrizations GRV94 [2], MRS(A) [3] and CTEQ [4] at different values of Q^2 as function of x_{Bj}). Data on photoproduction of J/Ψ seems to favor the MRS(A) parametrization [5]. This question, however, is still open.

We will argue that the large rapidity coverage collider detectors at the Tevatron offer an unique opportunity to measure the gluon structure function at $2 GeV^2 \leq Q^2 \leq m_b^2 + p_t^2$, where m_b is the b - quark mass and p_t is its transverse momentum, at $10^{-4} < x < 10^{-2}$ using the process of the diffractive dissociation of proton into $b\bar{b}$ - pair. This process lego plot and amplitude are pictured on Fig. 2 and Fig.3 respectively. It is clear from these figures that this process is a typical large rapidity gap (LRG) process, suggested by Bjorken [6]. As pointed out by Bjorken, and as we demonstrate below, such a process can be described as the exchange of a “hard” Pomeron, which could be rewritten through the gluon structure function due to the intimate relation between inelastic and elastic process given by the optical theorem (Fig.4), (see ref. [7] [8] for more details).

We will show that the cross section of the diffraction dissociation (DD) can be described as the sum of two different contributions *:

1. the first is proportional to the probability of finding a $b\bar{b}$ color dipole with a small size, of the order of $r_t^2 \propto \frac{1}{m_b^2 + p_t^2}$, in the fast hadron wave function before the interaction with the target. This dipole scatters with the target and produces the measured final state of the DD process. This mechanism has a normal partonic interpretation and, in the Bjorken frame for the projectile (in other words in the frame where the $b\bar{b}$ color dipole is at rest), it looks as a measurement of the partonic content of the Pomeron and corresponds to the Ingelman-Schlein (IS) hypothesis of the Pomeron structure function [9].

*In what follows we use at large the parton picture of interaction. It is easier to discuss the diffractive processes in this picture in the frame where the antiproton is at rest (the fixed target frame). Of course, all results will be given in relativistic invariant way.

2. the second is the production of the $\bar{b}b$ - pair after or during the interaction with a target. We will show that this mechanism corresponds to the so called coherent diffraction (CD) (see ref.[10]) and we will demonstrate that the measurement of the $\bar{b}b$ diffraction will allow, thanks to the the different dependance on the transverse momenta of produced quarks for both mechanisms, the separation of the CD contribution from the (IS) one.

We would like to stress that the above two contributions are closely related to the classic diffractive dissociation picture suggested by Good and Walker [11] 25 years ago. Indeed, there are two different possibilities for the dissociation of a hadron h into a pair of hadrons (h_1 and h_2): first, the beam particle (h) interacts with the target and dissociates into the pair of hadrons (h_1 and h_2); second, the beam particle dissociates first and one of the produced particle interacts with the target (see ref. [12] for details).

However, we will argue that the diffractive production of the heavy quark system is originated from the small distances where we can develop a theoretical approach based on perturbative QCD (pQCD). The pQCD approach allows us to calculate the diffractive dissociation process of $\bar{b}b$ in such details which are beyond our reach in “soft” high energy phenomenology.

2 Notations and kinematics.

1. $y = \frac{1}{2} \ln \frac{E+p_L}{E-p_L}$ is the rapidity of a particle with energy E and longitudinal momentum (along the beam direction) p_L . For the rapidity in the center of mass frame we use the notation y^* .

2. P_1 and P_2 are the momenta of colliding proton and antiproton (in the c.m. frame $P_1 = P_2$):

$$\begin{aligned} P_1 &= \left\{ \frac{\sqrt{s}}{2} \left(1 + \frac{2m^2}{s} \right), \frac{\sqrt{s}}{2}, 0, 0 \right\} ; \\ P_2 &= \left\{ \frac{\sqrt{s}}{2} \left(1 + \frac{2m^2}{s} \right), -\frac{\sqrt{s}}{2}, 0, 0 \right\} . \end{aligned} \tag{1}$$

3. y_1 and y_2 are the rapidities of produced b and \bar{b} quarks, p_{1t} and p_{2t} are their transverse momenta and m_b is the b mass.

4. M^2 is the mass of the produced $b\bar{b}$ -pair. m is the mass of the proton or antiproton. s is the squared energy of the reaction in the c.m. frame and it is equal to $s = (P_1 + P_2)^2$

5. $\Delta y = y_1 - y_2$ is the difference of rapidities between the produced b and \bar{b} .

6. $Y = \frac{y_1 + y_2}{2}$ is the mean rapidity of the $\bar{b}b$ system.

7. $m_{it}^2 = m_b^2 + p_{it}^2$ where $i = 1, 2$.

8. For the purpose of obtaining the kinematic relation in the simplest way we use the Sudakov decomposition [13] of the momenta of all particles, namely

$$p_{i\mu} = \alpha_i P_{1\mu} + \beta_i P_{2\mu} + p_{it\mu} , \quad (2)$$

where vector \vec{p}_{it} is orthogonal to $P_{1\mu}$ and $P_{2\mu}$.

At high energy $p_{i\mu}^2 = \alpha_i \beta_i s - p_{it}^2$ and the rapidity of particle "i" is equal to

$$y_i^* = \frac{1}{2} \ln \frac{\alpha_i}{\beta_i} . \quad (3)$$

9. Using Eqs.(1),(2) and (3) we obtain, for produced b quarks:

$$\alpha_1 = \frac{m_{1t}}{\sqrt{s}} e^{y_1^*} ; \quad \beta_1 = \frac{m_{1t}}{\sqrt{s}} e^{-y_1^*} ; \quad \alpha_2 = \frac{m_{2t}}{\sqrt{s}} e^{y_2^*} ; \quad \beta_2 = \frac{m_{2t}}{\sqrt{s}} e^{-y_2^*} . \quad (4)$$

and

$$M^2 = 2 m_{1t} m_{2t} \cosh(\Delta y) + m_{1t}^2 + m_{2t}^2 \quad (5)$$

10. Let us introduce x_1 - the energy fraction of hadron "1" carried by gluon k in Fig.3 and - the energy fraction of hadron "2" carried by the Pomeron with momentum q (gluon "ladder" in Fig.3). We show below that x_1, x_2 will be the arguments of the gluon structure functions in the cross section expression. Directly from Fig.3 one can see that

$$x_1 = \alpha_1 + \alpha_2 + \alpha_q ; \quad x_2 = \beta_1 + \beta_2 + \beta_k , \quad (6)$$

where (x_1, β_k) and (α_q, x_2) are the longitudinal components of the four momenta of gluon 1 and the Pomeron, respectively.

The main property of high energy scattering is the fact that $\alpha_q \ll \alpha_1$ and or α_2 and $\beta_k \ll \beta_1$ and or β_2 (see, for example, ref. [14]). Therefore, we can easily derive from eq. (6), assuming $m_{1t} = m_{2t}$:

$$x_1 = \frac{2 m_{1t}}{\sqrt{s}} e^{Y^*} \cosh\left(\frac{\Delta y}{2}\right) ; \quad x_2 = \frac{2 m_{1t}}{\sqrt{s}} e^{-Y^*} \cosh\left(\frac{\Delta y}{2}\right) . \quad (7)$$

11. Throughout the paper we will choose a frame where antiproton (see Fig.2 and Fig.3) is essentially at rest and where all momenta (l_i) of fast particles look as follows:

$$l_i = (l_{i+}, l_{i-}, \vec{l}_{it}) = \left(l_{i+}, \frac{m^2 + l_{it}^2}{l_{i+}}, \vec{l}_{it} \right) , \quad (8)$$

where $l_{i+} = l_{i0} + l_{i3}$ and $l_{i-} = l_{i0} - l_{i3}$.

12. $xG(x, Q^2)$ everywhere in the paper is the gluon structure function.

3 The value of the cross section in the generalized parton model.

From Figures 3 and 4 we can see that the value of the cross section of our process

$$p(P_1) + \bar{p}(P_2) \rightarrow b(y_1, p_{1t}) + \bar{b}(y_2, p_{2t}) + X + [LRG(Y)] + \bar{p}(P_2 - q) \quad (9)$$

is equal to

$$\frac{d\sigma}{dY dq_t^2 d\Delta y dp_t^2} \Big|_{q_t^2=0} = (x_1 G(x_1, \mu^2)) \frac{d\sigma^G}{dY dq_t^2 d\Delta y dp_t^2} \Big|_{q_t^2=0}, \quad (10)$$

where σ^G is the reaction cross section.

$$G(x_1, k_t^2) + \bar{p}(P_2) \rightarrow b(y_1, p_{1t}) + \bar{b}(y_2, p_{2t}) + [LRG(Y)] + \bar{p}(P_2 - q) \quad (11)$$

The physical meaning of eq. (10) is very simple: $x_1 G(x_1, \mu^2)$ is the probability of finding a gluon with the fraction of energy x_1 inside of the proton and σ^G is the cross section of its interaction with the antiproton. In the spirit of the factorization theorem [15] we introduce the factorization scale μ^2 , the maximal value of k_t^2 at which we still can neglect the dependence of σ^G on k_t^2 .

To simplify the color algebra we adopt throughout the paper the colorless probe approach, replacing the gluon with the transverse momentum k_t and the fraction of energy x_1 by a colorless probe with the same kinematics. The physical motivation is clear and based on the factorization equation (eq. (10)). Indeed, we can measure the gluon structure function using a colorless probe like the graviton or heavy Higgs boson. The properties of such a probe have been studied in details in ref. [16].

The cross section for the reaction of eq. (11) can be easily calculated. It is clear that we have two mechanisms for $\bar{b}b$ -production by the colorless probe which we will discuss in the rest target rest frame (antiproton in Fig.2).

1. The first mechanism is the following: there is a $\bar{b}b$ component in the wave function of the fast probe before its interaction with the target. This $\bar{b}b$ pair is a color dipole with sufficiently small transverse size of the order of $r_t^2 \propto \frac{1}{m_b^2 + p_t^2}$ which scatters with the target producing the measured final state.

2. The second mechanism is the production of the $\bar{b}b$ - pair after or during the interaction with the target.

These two mechanisms correspond to the two set of the Feynman diagrams pictured in figures 5a and 5b, respectively.

Let us start from the first one which looks normal from partonic point of view in the sense that, in the Bjorken frame for the probe, it looks like the measurement of the partonic content of the Pomeron and corresponds to the Ingelman - Schlein hypothesis of the Pomeron structure function [9]. For the set of the Feynman diagrams of Fig. 5a the amplitude of $\bar{b}b$ production can be written as a product of two factors: (i) the wave function of $\bar{b}b$ pair in a virtual gluon $\Psi_{\lambda_1\lambda_2}^{G^*}$ and (ii) the rescattering amplitude of the quark - antiquark pair on the target $T_{\lambda_1\lambda_2}$, where λ_i is the quark polarization. Following the conventions of ref.[17], we have:

$$M_f = \sqrt{N_c} \int \frac{d^2 p'_t}{16\pi^3} \int_0^1 dz' \Psi_{\lambda_1\lambda_2}^{G^*}(p'_t, z') T_{\lambda_1\lambda_2}(p'_t, z'; p_t, z), \quad (12)$$

where p_t is the transverse momentum of the produced quark and z is the fraction of energy carried by b -quark with respect to energy of the gluon. It is easily found from eq. (4) and eq. (6) that

$$z = \frac{\alpha_1}{x_1} = \frac{\alpha_1}{\alpha_1 + \alpha_2 + \alpha_q} = \frac{e^{\frac{\Delta y}{2}}}{e^{\frac{\Delta y}{2}} + e^{-\frac{\Delta y}{2}}}, \quad (13)$$

where α_q we can be found from the equation: $(P_2 - q)^2 = m^2$ and it is equal to $\alpha_q = \frac{q^2}{(1-x_2)s} \ll \alpha_1 + \alpha_2$ at large s . In deriving eq. (13) we have also assumed that $\vec{p}_{1t} = -\vec{p}_{2t} + \vec{k}_t + \vec{q}_t \rightarrow -\vec{p}_{2t}$.

The virtual gluon breaks into a quark - antiquark pair with a large lifetime which is equal to τ_{G^*} . In leading $\log(1/x)$ approximation of pQCD, which we will use here, the time of interaction is much smaller than τ_{G^*} and during this time the exchange of gluons does not change the fraction of energy carried by quark or/and antiquark. It is instructive to recall the argument of why this is so. According to the uncertainty principle the lifetime of the $\bar{b}b$ fluctuation (τ_{G^*}) is

$$\tau_{G^*} \sim \frac{1}{\Delta E} = \left| \frac{1}{k_- - p_{1-} - p_{2-}} \right| = \frac{x_1 z(1-z) P_{1+}}{m_t^2 + z(1-z)k_t^2}. \quad (14)$$

An estimate of the interaction time can be obtained from the typical time for the emission of a gluon with momentum l , from the quark p_1 , say. Then

$$\tau_i \sim \left| \frac{1}{p'_{1-} - p_{1-} - l_-} \right| = \left| \frac{x_1 P_{1+}}{\frac{m_t^2}{z'} - \frac{m_t^2}{z} - \frac{l_t^2}{\alpha_l}} \right|, \quad (15)$$

where $\alpha_l = \frac{l_+}{x_1 P_{1+}}$ and $z' = z + \alpha_l$. In the leading $\log(1/x)$ approximation of pQCD we have $\alpha_l \ll z$ and hence

$$\tau_i \approx \frac{\alpha_l x_1 P_{1+}}{l_t^2} \ll \tau_{G^*}. \quad (16)$$

Therefore, the interaction only changes the transverse momenta of quarks (see Fig.3). The vertices also do not depend on the type of the diagram since the exchange of gluons preserves helicity at high energy. Finally the amplitude T can be reduced to the form [17]:

$$T_{\lambda_1 \lambda_2} = \quad (17)$$

$$= 16\pi^3 \int \{ 2\delta(\vec{k}'_t - \vec{k}_t) - \delta(\vec{k}'_t - \vec{k}_t - \vec{l}_t) - \delta(\vec{k}'_t - \vec{k}_t + \vec{l}_t) \} \cdot \delta(z - z') \phi(l_t, x) \frac{d^2 l_t d l_+}{16\pi^3 l_t^4},$$

where the function ϕ corresponds to the “ladder” diagram (see Fig.3) and only weakly (logarithmically) depends on l_t . l_+ is the large component of vector l_μ which we have introduced in the previous section. The difference in signs between the terms in Eq.(17) reflects the different color charge of quark and antiquark.

Substituting eq. (17) in eq. (12) we obtain:

$$M_f = \sqrt{N_c} \int \Delta \Psi_{\lambda_1 \lambda_2}^{G^*}(p_t, l_t, z) \phi(l_t, x) \frac{d^2 l_t d l_+}{16\pi^3 l_t^4} \quad (18)$$

where

$$\Delta \Psi^{G^*}(p_t, l_t, z) = 2 \Psi^{G^*}(p_t, z) - \Psi^{G^*}(p_t - l_t, z) - \Psi^{G^*}(p_t + l_t, z). \quad (19)$$

Function Ψ has been found to be (see for example ref. [17]):

$$\Psi_{\pm}^{G^*}(p_t, z) = -g \frac{\bar{u}_{\lambda_1}(p_1) \vec{\gamma} \cdot \vec{\epsilon}^{G^*} v_{\lambda_2}(p_2)}{\sqrt{z(1-z)} (k^2 - \frac{m_b^2 + p_t^2}{z(1-z)})} = \quad (20)$$

$$= -g \cdot \frac{1}{a^2 + p_t^2} \{ \delta_{\lambda_1 - \lambda_2} [\lambda_1 (1 - 2z) \pm 1] \vec{\epsilon}_{\pm}^{G^*} \cdot \vec{p}_t \pm m_b \delta_{\lambda_1 \lambda_2} \}$$

where $\alpha_S = \frac{g^2}{4\pi}$; $\vec{\epsilon}_{\pm}^{G^*}$ is the circular polarization vector of the gluon ($\vec{\epsilon}_{\pm}^{G^*} = \frac{1}{\sqrt{2}}(0, 1, \pm 1, 0)$) and $a^2 = m_b^2 + k^2 z(1-z)$. We have used formulae from refs.[18] and [16] in the above calculations.

Considering $l_t^2 \ll m_{b_t}^2$ we obtain :

$$\Delta \Psi_{\pm}^{G^*}(p_t, l_t, z) = -2g \cdot l_t^2 \cdot \quad (21)$$

$$\cdot \{ 4 \frac{a^2}{(a^2 + p_t^2)^3} \delta_{\lambda_1 \lambda_2} [\lambda_1 (1 - 2z) \pm 1] \vec{\epsilon}_{\pm}^{G^*} \cdot \vec{p}_t + m_b \frac{a^2 - p_t^2}{(a^2 + p_t^2)^3} \pm \delta_{\lambda_1 - \lambda_2} \}.$$

In the leading log approximation in $\ln(1/x)$ and $\ln(a^2/\Lambda^2)$ [19, 17]

$$\int \phi(l_t, x) \frac{d^2 l_t d l_+}{16\pi^3 l_t^4} = i \frac{4\pi^2 T_{R\alpha S}}{N_c} (s + k^2) x G(x, a^2 + p_t^2), \quad (22)$$

where T_R/N_c arises from averaging over colors ($T_R = 1/2$).

Collecting all previous equations we can calculate cross section:

$$\frac{d\sigma^G}{dY dq_t^2 d\Delta y dp_t^2} \Big|_{q_t^2=0} = \frac{\sum_{\lambda_1 \lambda_2} M_f^2}{16\pi s^2} \frac{dz}{d\Delta y} = \frac{dz}{d\Delta y} \alpha \alpha_S^2 \frac{16\pi^2}{9}. \quad (23)$$

$$\cdot \left\{ [(z^2 + (1-z)^2) p_t^2] \left(\frac{a^2}{(a^2 + p_t^2)^3} \right)^2 + \frac{1}{4} m_b^2 \left(\frac{a^2 - p_t^2}{(a^2 + p_t^2)^3} \right)^2 \right\} \cdot (xG(x, a^2 + p_t^2))^2$$

Finally, we can rewrite eq. (23) in the form ($N_c = 3$):

$$\frac{d\sigma^G}{dY dq_t^2 d\Delta y dp_t^2} \Big|_{q_t^2=0} = \quad (24)$$

$$= \frac{16\pi^2 \alpha_S^3}{9} \frac{1}{4 \cosh^2(\frac{\Delta y}{2})} \left[\frac{\cosh(\Delta y)}{2 \cosh^2(\frac{\Delta y}{2})} p_t^2 + \frac{m_b^2}{4} \left(1 - \frac{p_t^2}{a^2} \right)^2 \right] \cdot \left\{ \frac{a^2}{(a^2 + p_t^2)^3} \right\}^2 (xG(x, a^2 + p_t^2))^2.$$

For the cross section of the diffractive dissociation we have (after sum over gluon polarization and correct averaging over color ($N_c = 3$)):

$$\frac{d\sigma}{dY dq_t^2 d\Delta y dp_t^2} \Big|_{q_t^2=0} = (x_1 G(x_1, \mu^2)) \cdot \quad (25)$$

$$\cdot \frac{16\pi^2 \alpha_S^3}{9} \frac{1}{4 \cosh^2(\frac{\Delta y}{2})} \left[\frac{\cosh(\Delta y)}{2 \cosh^2(\frac{\Delta y}{2})} p_t^2 + \frac{m_b^2}{4} \left(1 - \frac{p_t^2}{a^2} \right)^2 \right] \cdot \left\{ \frac{a^2}{(a^2 + p_t^2)^3} \right\}^2 (x_2 G(x_2, a^2 + p_t^2))^2$$

From the expression for a we can set the factorization scale, since our cross section ceases to depend on k_t^2 if $k_t^2 \leq 4m_{bt}^2$. Therefore, the reasonable choice is $\mu^2 = 4m_{bt}^2$. We can neglect the scale dependance in our cross section and put $a^2 = m_b^2$. All ingredients of Eq.(25) are clearly seen in Fig. 6.

Taking into account the running QCD coupling constant we have to replace α_S^3 in Eq.(25) by $\alpha_S(\mu^2)\alpha_S^2(a^2 + p_t^2)$.

Now, let us consider the diagrams of Fig. 5b. They correspond to the possibility of producing a $\bar{b}b$ pair inside of the Pomeron. Indeed, the Pomeron is not a point-like particle; gluons inside it live sufficiently long time and during this time they can create a $\bar{b}b$ -pair which rescatters with the proton by exchange only one gluon. Indeed, the lifetime of $G_l G_l$ - pair in the diagram of Fig. 5b is equal to $\tau_l = \frac{x_1 s}{k_t^2 + \frac{l_t^2}{z_l(1-z_l)}}$, where z_l is the

energy fraction of gluon l . This time is much bigger than the time τ_b that $\bar{b}b$ - pair lives ($\tau_b = \frac{x_1 s}{M^2} \ll \tau_l$).

As has been discussed many times (see, for example refs. [16] [20] [21]) we can safely calculate the diagram of fig. 5b by closing the contour of integration over β_l on the propagator marked by cross in Fig. 5b. We anticipate that $l_t < k_t$ and that the vertex of emission of the gluon $1'$ is proportional to $l_{\mu t}$ (see ref.[14]). The interaction of the gluon with transverse momentum $k_t + l_t$ with the target is calculated using eq. (18) with

$$\Delta\Psi(p_t, l_t, z) = \Psi(p_t + l_t, z) - \Psi(p_t - l_t, z) . \quad (26)$$

Substituting eq. (20) in eq. (26) one obtains after integration over the azimuthal angle of vector l_t :

$$\begin{aligned} \Delta\Psi(p_t, l_t, z) &= -2g l_t^2 \vec{p}_t \cdot \\ &\cdot \left\{ \delta_{\lambda_1 - \lambda_2} [(1 - 2z)\lambda_1 \pm 1] \frac{a^2}{(a^2 + p_t^2)^2} - \delta_{\lambda_1 \lambda_2} m_b \lambda_1 \frac{1}{(a^2 + p_t^2)^2} \right\} . \end{aligned} \quad (27)$$

Using eq. (22) and eq. (23) we obtain ($N_c = 3$):

$$\begin{aligned} &\frac{d\sigma^{G^*}[CD]}{dY dq_t^2 d\Delta y dp_t^2} \Big|_{q_t^2=0} = \\ &= \frac{4\pi^2 \alpha_S^3}{9} \frac{1}{4 \cosh^2(\frac{\Delta y}{2})} \left[\frac{\cosh(\Delta y)}{2 \cosh^2(\frac{\Delta y}{2})} a^4 + m_b^2 p_t^2 \right] \cdot \frac{1}{k_t^2} \cdot \left\{ \frac{1}{(a^2 + p_t^2)^2} \right\}^2 (x_2 G(x_2, k_t^2))^2 . \end{aligned} \quad (28)$$

Notice that extra factor $1/k_t^2$ in eq. (28) comes from the fact that $\Delta\Psi$ of eq. (27) does not depend on the polarization of the gluon with transverse momentum k_t which is proportional to k_t and cancels one of the gluon propagators in eq. (23). We would like to recall that in the previous calculation we assumed that $l_t < k_t$ and this inequality establish the scale in the gluon structure function in eq. (28). The answer for the cross section of the coherent diffraction has the form:

$$\begin{aligned} &\frac{d\sigma[CD]}{dY dq_t^2 d\Delta y dp_t^2} \Big|_{q_t^2=0} = \int^{m_{bt}^2} \frac{dk_t^2}{k_t^4} \frac{\partial x_1 G(x_1, k_t^2)}{\partial \ln k_t^2} (x_2 G(x_2, k_t^2))^2 \cdot \\ &\cdot \frac{4\pi^2 \alpha_S^3(k_t^2)}{9} \frac{1}{4 \cosh^2(\frac{\Delta y}{2})} \cdot \left[\frac{\cosh(\Delta y)}{2 \cosh^2(\frac{\Delta y}{2})} a^4 + m_b^2 p_t^2 \right] \cdot \frac{1}{(a^2 + p_t^2)^4} . \end{aligned} \quad (29)$$

This equation gives the contribution for so called coherent diffraction (CD) [10]. The most contribution to the integral comes from the region of sufficiently small k_t due to the factor k_t^4 in the dominator and for the proton $k_t \propto \frac{1}{R_p}$ where R_p is the proton radius. It means

that we cannot trust our perturbative calculation for the CD contribution. However, if we calculate the integral

$$\int^{m_{bt}^2} \frac{dk_t^2}{k_t^4} \frac{\partial x_1 G(x_1, k_t^2)}{\partial \ln k_t^2} (x_2 G(x_2, k_t^2))^2, \quad (30)$$

using the current parametrization of the gluon structure function, we can find out that the typical k_t^2 , which is essential in the integral, is not very small but about $1 - 2 \text{ GeV}^2$. To understand this fact we have to remember that the gluon structure function behaves as $(k_t^2)^{<\gamma>}$ (at least in semiclassical approach) and the value of $<\gamma>$ calculated in the current parametrization for the gluon structure function turns out to be rather big in the region of $k^2 \approx 1 - 2\text{GeV}^2$ (see Fig. 9). One can see that if $<\gamma> > 0.5$ the integral converges on the upper limit or, in other words, the small distances start to be important.

To check this statement we calculate the integrand of eq. (30) as a function of $\ln(k_t^2/Q_0^2)$ with $\frac{\partial x_1 G(x_1, k_t^2)}{\partial \ln k_t^2} = 1$. $Q_0^2 = 0.34 \text{ GeV}^2$ is the initial virtuality in the GRV parametrization. The result of the calculation is plotted in Fig. 8a for the GRV, in Fig. 8b for the MRS(A') and in Fig. 8c for the CTEQ parametrizations. We see a definite maximum in $\ln k_t^2/Q_0^2$ dependence around $k_t^2 \approx 1 - 1.5\text{GeV}^2$ which becomes more pronounced at smaller values of x_2 . It means that we can safely use the perturbative QCD approach to calculate the CD contribution.

In numerical estimates of eq. (29) we use the GLAP equation [24] to calculate $\frac{\partial x_1 G(x_1, k_t^2)}{\partial \ln k_t^2}$, namely :

$$\begin{aligned} \frac{\partial x_1 G(x_1, k_t^2)}{\partial \ln k_t^2} = & \frac{\alpha_S(k_t^2)}{2\pi} \left\{ \frac{4}{3} \int_x^1 \frac{dz}{z} [z^2 + 2(1-z)] \sum_i \frac{x}{z} q_i\left(\frac{x}{z}, k_t^2\right) + \right. & (31) \\ & + 6 \int_x^1 \frac{dz}{z} [z^2(1-z) + 1-z] \frac{x}{z} G\left(\frac{x}{z}, k_t^2\right) + 6 \int_x^1 \frac{zdz}{1-z} \left[\frac{x}{z} G\left(\frac{x}{z}, k_t^2\right) - xG(x, k_t^2) \right] + \\ & \left. + 6 \left[\frac{11}{12} - \frac{N_f}{18} \right] xG(x, k_t^2) \right\}, \end{aligned}$$

where N_f is the number of flavours and $N_C = 3$ is the number of colors. The running coupling QCD constant $\alpha_S(k_t^2) = \frac{4\pi}{(11 - \frac{2}{3}N_f) \ln \frac{k_t^2}{\Lambda^2}}$.

It is worthwhile mentioning that in the case of the diffractive dissociation in the deep inelastic scattering the smallest value of k_t is $k_t^2 = Q^2$ and eq. (29) gives the contribution of the order of $1/Q^2$. In other words, the coherent diffraction in this case is a high twist contribution while the (IS) diffraction (see eq. (25)) occurs in the leading twist. This result has been obtained in ref. [22].

It should be stressed that there is no interference between the Ingelman-Schlein and the coherent diffraction contributions. Indeed, the interference term vanishes due to integration over the azimuthal angle of p_t and summation over gluon polarizations, as one can see comparing Eq.(21) and Eq.(27)

4 Numerical estimates.

Setting $x_1 = 0.1$ we can estimate $x_2 \approx 0.6 \cdot 10^{-3}$. As far as the value of the cross section is concerned, we get at $\Delta y = 0$ and $p_t = 0$ the value (at $\alpha_S = 0.25$)

$$\frac{d\sigma}{dY dq_t^2 d\Delta y dp_t^2} \Big|_{q_t^2=0} \approx 0.1 \cdot 10^{-3} \frac{mbarn}{GeV^4}$$

Here, we took $x_2 G(x_2, m_{bt}^2) = 20$, which is the value in the GRV parametrization.

The result of a detailed calculation is presented in Fig. 10. To test the sensitivity of our result to high order QCD corrections we plotted the cross section for the coherent diffraction for two cases: fixed and running QCD coupling constant. The difference is rather big but it does not change the main conclusion: the coherent diffraction gives much bigger cross section than the Ingelman-Schlein contribution of Eq.(25). (IS in Fig. 9a). Therefore, the measurement of the diffractive dissociation in $b\bar{b}$ system gives the unique opportunity to study the CD unlike the deep inelastic processes where the CD is suppressed.

One can see from Fig. 9b that the value of the differential cross section crucially depends on the parametrization of the gluon structure function with the difference about factor 2. This difference encourages us to claim that the measurement of the $b\bar{b}$ diffractive production could provide the selection of the parameterization and give an important contribution to the extraction of the value of the gluon structure function from experiment.

We also calculate the integrated cross section defined as

$$\frac{d\sigma}{dY} = \int_{p_t^{min}}^{\infty} dp_t^2 \int_{-\infty}^{+\infty} d\Delta y \int_0^{\infty} dq_t^2 \frac{d\sigma}{dY d\Delta y dq_t^2 dp_t^2} , \quad (32)$$

The value of p_t^{min} can be taken from the experimental values obtained by the Tevatron Collider experiments. In reference Ref. [25] analysis techniques are used to separate muons coming from different sources and, in particular, from $b \rightarrow \mu + \nu + c$ process for $p_t^{min} \geq 5$ GeV. We assumed, in the integration over q_t^2 , an exponential behaviour of $d\sigma$ with respect to q_t^2

$$\frac{d\sigma}{dq_t^2} = \frac{d\sigma}{dq_t^2} \Big|_{q_t^2=0} e^{-bq_t^2} \quad (33)$$

We take the slope $b = 4.9 \text{ GeV}^{-2}$ as it has been measured at HERA [23]. In our estimates we took $\alpha_S = 0.25$ which corresponds to the value of the running QCD coupling constant ($\alpha_S(k^2)$) at $k^2 \sim m_b^2$.

Fig. 10 shows that the value of the integrated cross section is not very small and can be measured by the Tevatron detectors in the next run. One can also see that the differences between the estimates in different parameterizations is rather big. It is about a factor 2-3 between the highest values of the cross section in the GRV parameterization and the lowest one in the MRS(A') parameterization.

Finally, we would like to stress that the Tevatron provides an unique possibility to look inside the microscopic mechanism of diffractive dissociation by measuring the coherent diffraction which gives a small contribution to the deep inelastic processes. The formulae written in this paper give us the basis for the Monte Carlo simulation of the diffractive events in 3-dimension phase space (η, ϕ, p_t) which we are going to present in further publications. This Monte Carlo will provide a more detailed estimates of the experimental possibilities at the Tevatron and, we hope, will encourage future experiments on large rapidity gap physics. We firmly believe that the diffractive dissociation opens a new window to study such difficult questions as the Pomeron structure, the matching between hard and soft processes and the search of new collective phenomena in QCD related to the high density parton system. We thank the Fermilab Theory, Computing and Research Divisions for the hospitality. E.L. is very grateful to LAFEX-CBPF/CNPq for the support and warm atmosphere during his stay in Brazil. We would like to thank H.Montgomery for fruitful discussions in Rio, and to Helio da Motta for reading the manuscript.

References

- [1] ZEUS collaboration, M. Derrick et.al.: *Z. Phys.* **C65** (1995) 379;
H1 collaboration, T.Ahmed et.al.: *Nucl. Phys.* **B439** (1995) 471;
ZEUS collaboration, M. Derrick et.al.: *Z. Phys.* **C68** (1995) 569;
H1 collaboration, T.Ahmed et.al.: *Phys. Lett.* **B348** (1995) 681.
- [2] M. Glück, E.Reya and A. Vogt: *Z. Phys.* **C67** (1995) 433.
- [3] A.D.Martin, R.G. Roberts and W.J. Stirling: *Phys. Lett.* **B354** (1995) 155.

- [4] H.L. Lai, et. al., CTEQ collaboration: *Phys. Rev.* **D51** (1995) 4763
- [5] M.G.Ryskin et.al: Durham University preprint, DTP/95/96, November 1995.
- [6] Yu.L. Dokshitzer, V.A. Khoze and T.Sjostrand: *Phys. Lett.* **B274** (1992) 116;
J.D. Bjorken: *Phys. Rev.* **D45** (1992) 4077; *Phys. Rev.* **D47** (1992) 101; *Nucl. Phys.*
B (Proc. Suppl.) **23C** (1992) 250; *Acta Phys. Pol.* **B23** (1992) 637.
- [7] M.Albrow et.al.: “*Future Experimental Studies of QCD at Fermilab: report of the QCD section: option for a Fermilab Strategic Plan*” FERMILAB-FN 622, Aug.1994.
- [8] A.H. Mueller, B. Müller, C. Rebbi and W.H. Smith: “Report of the DPF Long Range Planning Group on QCD”.
- [9] G. Ingelman and P.Schlein: *Phys. Lett.* **B152** (1985) 256.
- [10] J. Collins, L. Frankfurt and M. Strikman: *Phys. Lett.* **B307** (1993) 161.
- [11] M.L.Good and W.D.Walker: *Phys. Rev.* **120** (1960) 1857
- [12] G. Cohen Tannoudji, A. Santoro and M. Souza: *Nucl. Phys.* **B125** (1977) 445;
E.L.Berger and P.Pirila: *Phys. Rev.* **D12** (1975) 3448; *Phys. Lett.* **B59** (1975) 361;
E.L.Berger and R.Cutler: *Phys. Rev.* **D15** (1977) 1903;
G.Alberi and G.Goggi: *Phys. Rep.* **74** (1981) 1 and references therein.
- [13] V.V. Sudakov: *ZhETF* **30**(1956) 187.
- [14] L. V. Gribov, E. M. Levin and M. G. Ryskin: *Phys.Rep.* **100** (1983) 1.
- [15] J. Collins, D.E. Soper and G. Sterman: *Nucl. Phys.* **B308** (1988) 833; In *Perturbative Quantum Chromodynamics*, ed. A.H. Mueller. Singapore: World Scientific (1989) and reference therein.
- [16] A.H. Mueller: *Nucl. Phys.* **B335** (1990) 115;
- [17] S.J. Brodsky et al: *Phys. Rev.* **D50** (1994) 3134.
- [18] S.J.Brodsky and G.P.Lepage: *Phys. Rev.* **D22** (1980) 2157
- [19] E.M. Levin and M.G.Ryskin: *Sov. J. Nucl. Phys.* **45** (1987) 150.
- [20] E.A. Kuraev, L.N. Lipatov and V.S. Fadin: *Sov. Phys. JETP* **45** (1977) 199 ; Ya.Ya. Balitskii and L.V. Lipatov: *Sov. J. Nucl. Phys.* **28** (1978) 822; L.N. Lipatov: *Sov. Phys. JETP* **63** (1986) 904;
J.Bartels: *Nucl. Phys.* **B175** (1980) 365;
J. Kwiecinski: *Phys. Lett.* **B94** (1980) 413.

- [21] E. Levin and M. Wüsthoff: *Phys. Rev.* **D50** (1994) 4306.
- [22] E. Levin: “*Deep Inelastic Scattering and Related Subjects*” Eilat, Israel, 6-11 February 1994, ed. Aharon Levy, WS, 1994, p.83;
A. Berrera and D. Soper: *Phys. Rev.* **D50** (1994) 4328.
- [23] H1 collaboration. A. De Roeck et al.: DESY 95 - 52, August 1995.
ZEUS collaboration. M.Derrick et al.: DESY 95 - 133, July 1995.
- [24] V.N.Gribov and L.N. Lipatov: *Sov.J.Nucl.Phys.* **15** (1972) 438; L.N. Lipatov: *Yad. Fiz.* **20** (1974) 181; G. Altarelli and G. Parisi: *Nucl. Phys.* **B126** (1977) 298; Yu. L. Dokshitser: *Sov. Phys. JETP* **46** (1977) 641.
- [25] D0 Collaboration, S.Abachi et al., *Phys. Rev. Lett.* **74** (1995) 3548, and CDF Collaboration, F.Abe et al., *Phys. Rev. Lett.* **75** (1995) 1451

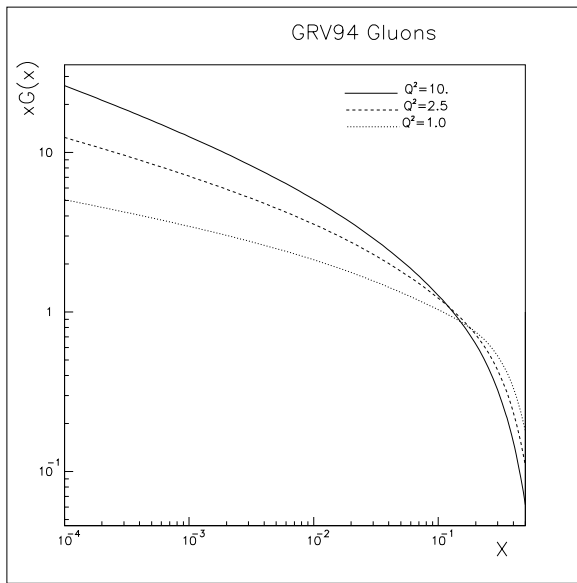


Fig.1a

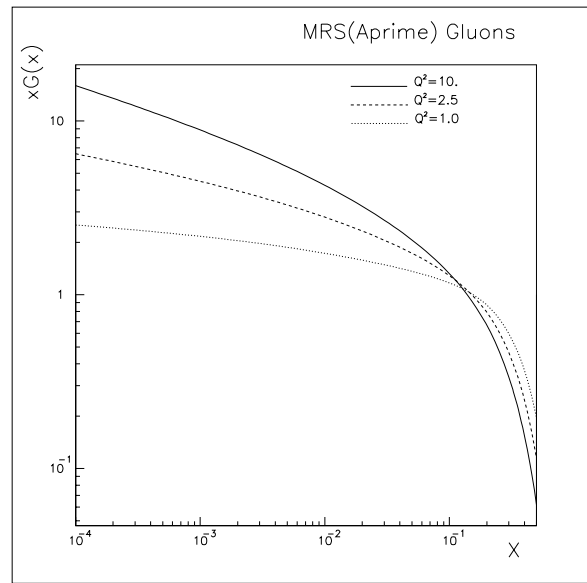


Fig.1b

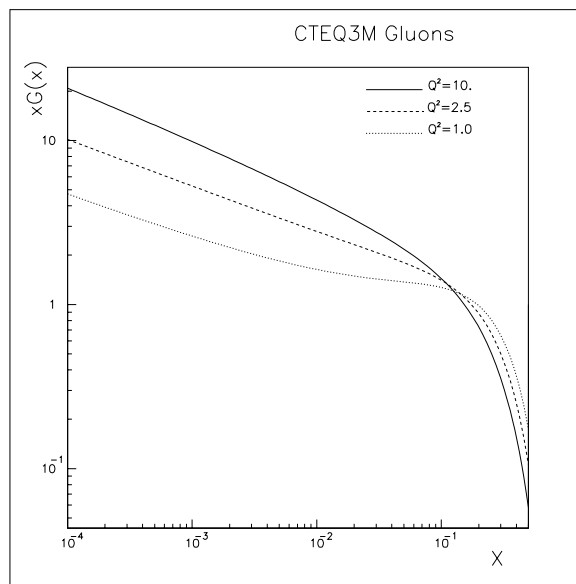


Fig.1c

Figure 1: Gluon structure function $xG(x, Q^2)$ in different parameterizations: GRV [2] (Fig.1a), MRS(A') [3] (Fig.1b) and CTEQ [4] (Fig.1c).

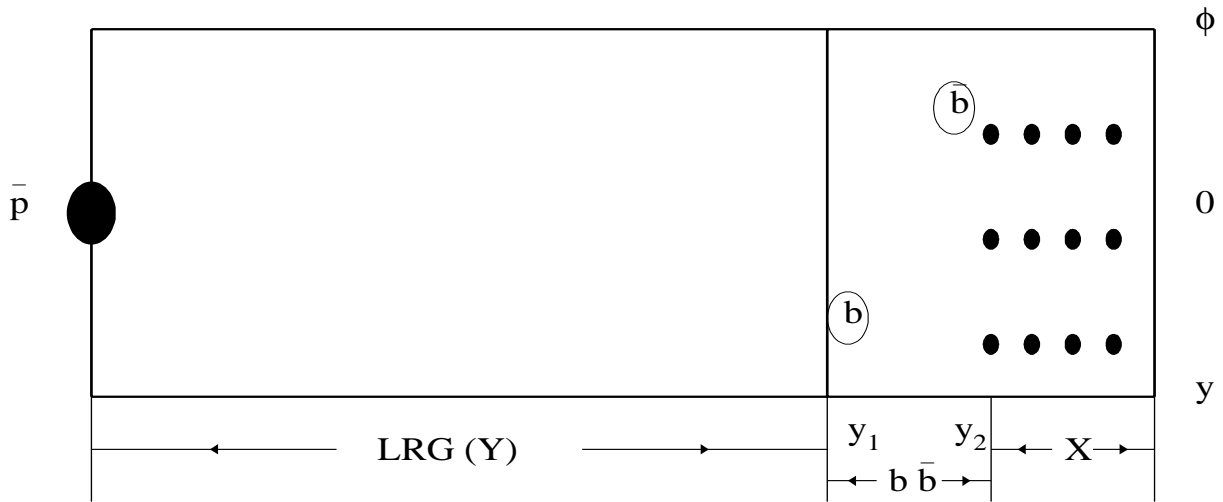


Figure 2: Lego - plot of $b\bar{b}$ diffractive production in $p\bar{p}$ collision.

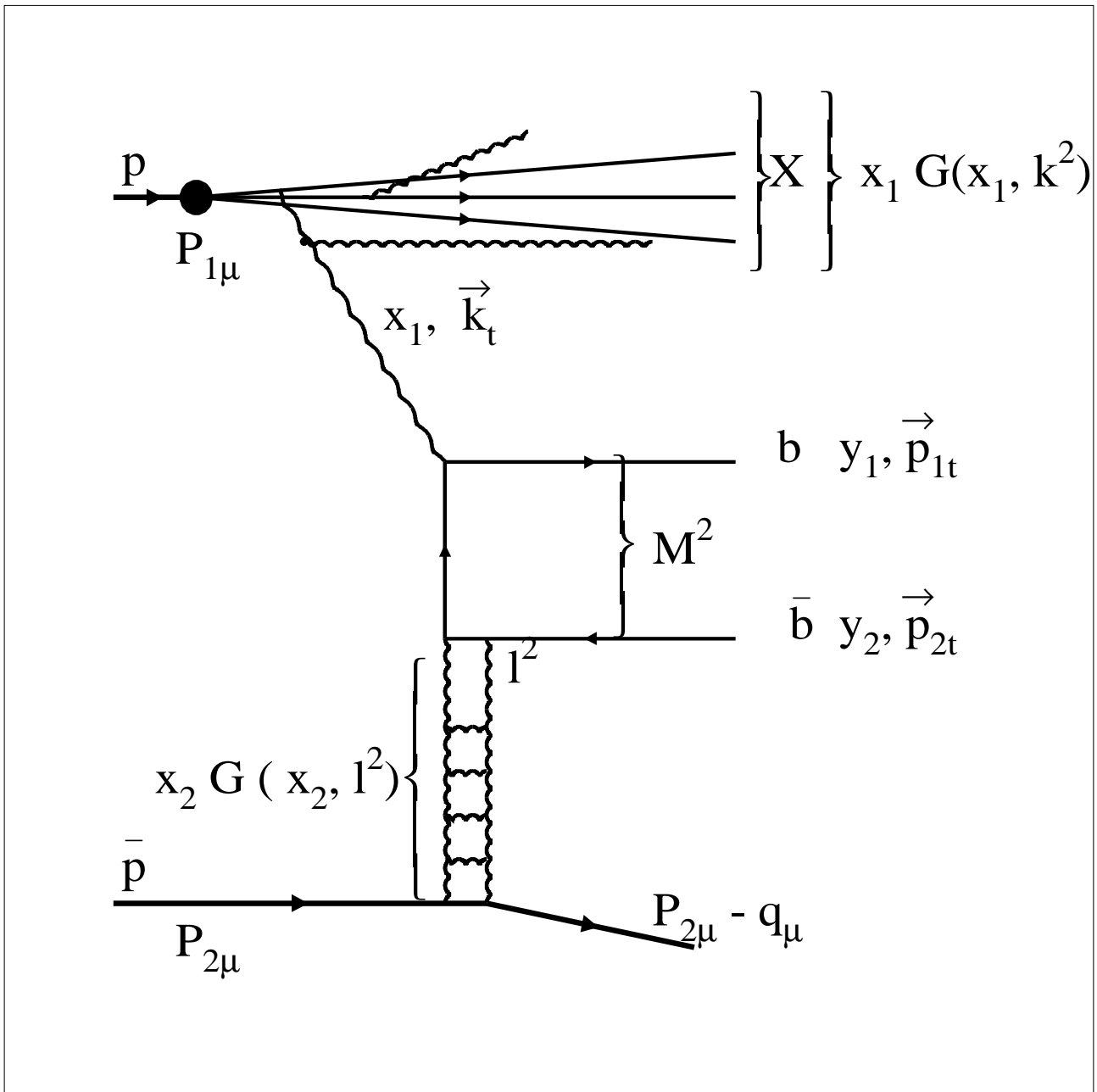


Figure 3: Amplitude of $b\bar{b}$ - diffractive production.

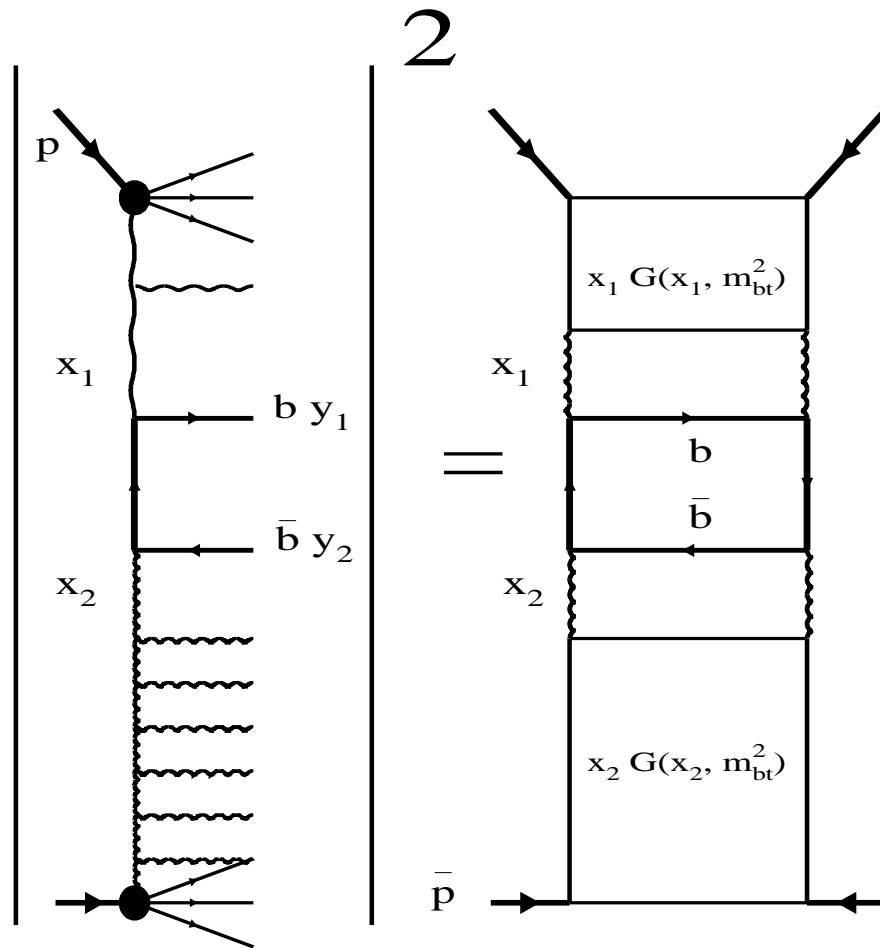


Figure 4: Optical Theorem.

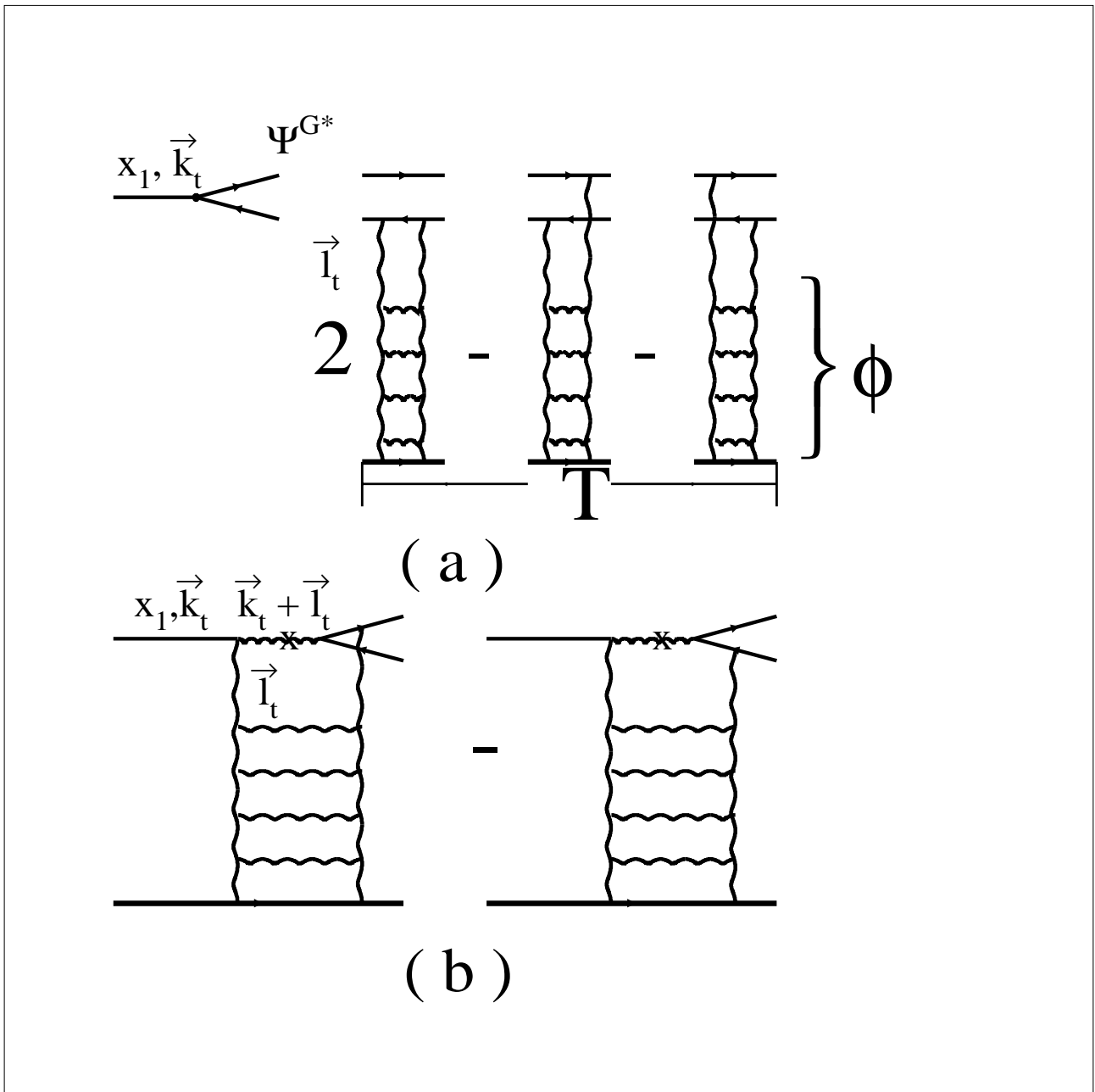


Figure 5: Feynman diagrams for $b\bar{b}$ diffractive production by colorless gluon probe.

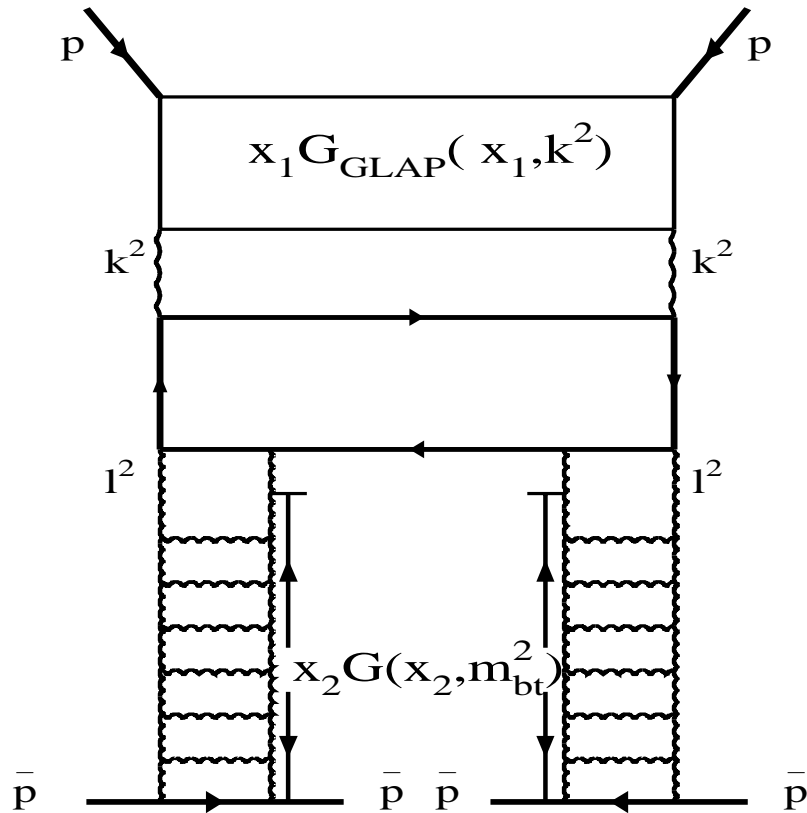


Figure 6: The cross section for $b\bar{b}$ diffractive production in the Ingelman - Schlein approach [9].

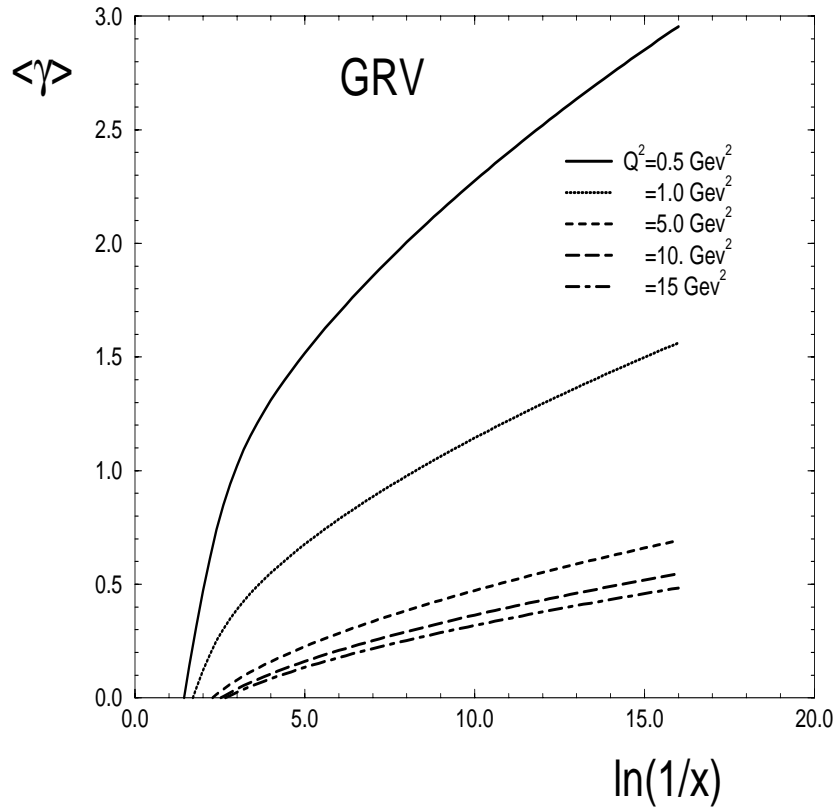


Figure 7: The behaviour of average $\langle \gamma \rangle$ for the GRV parameterization of the gluon structure function.

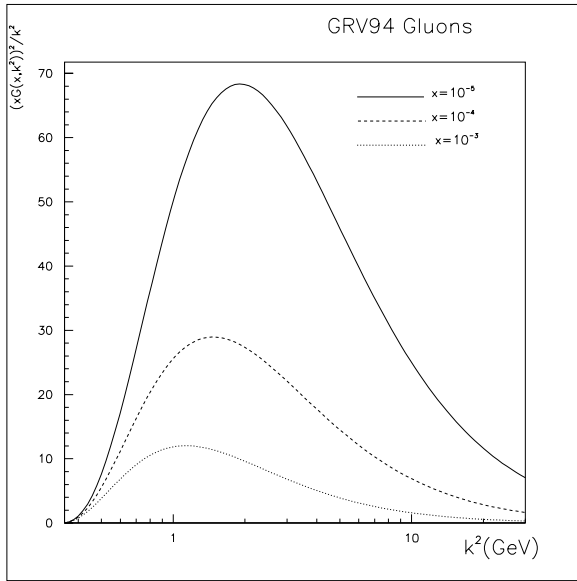


Fig. 8a

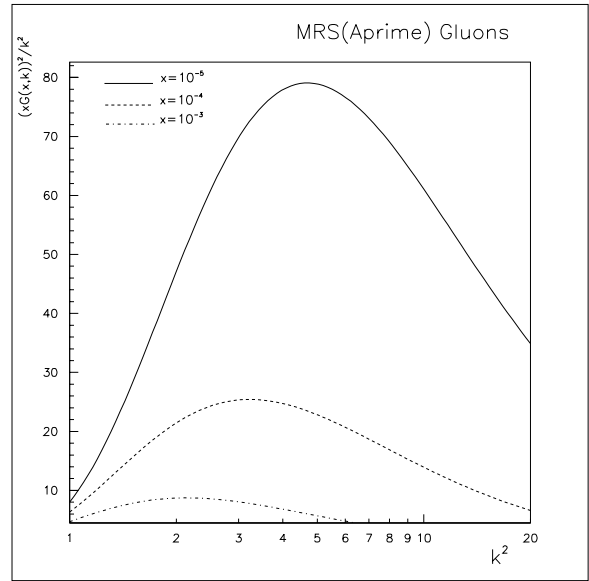


Fig.8b

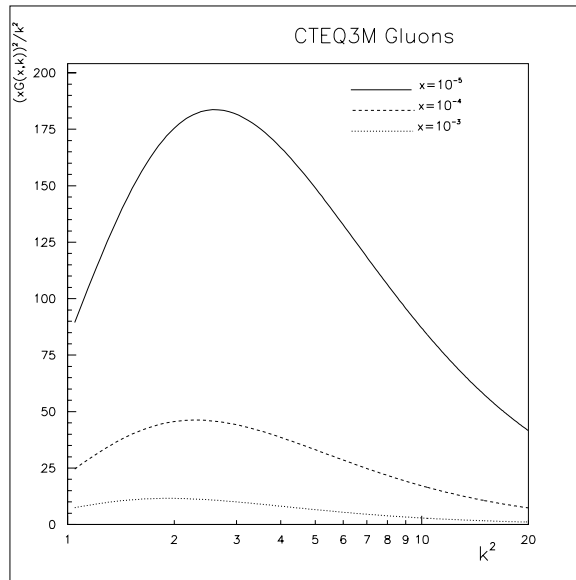


Fig.8c

Figure 8: $\frac{(x_2 G(x_2, k_t^2))^2}{k_t^2}$ versus $\ln(k_t^2/Q_0^2)$ in different parameterizations: GRV [2] (Fig.1a), MRS(A') [3] (Fig. 1b) and CTEQ [4] (Fig. 1c).

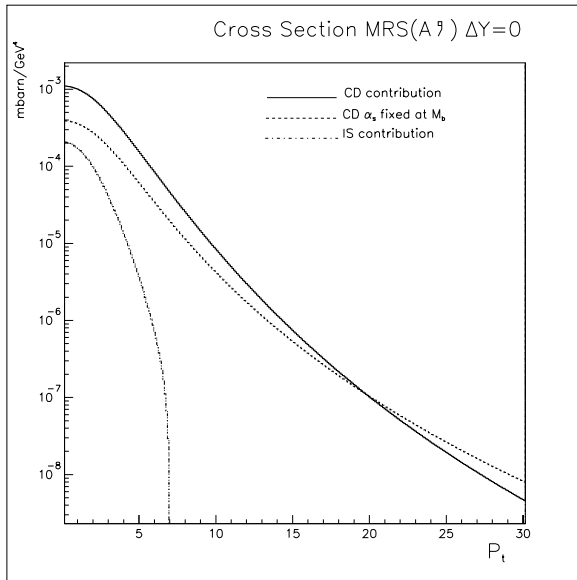


Fig. 9a

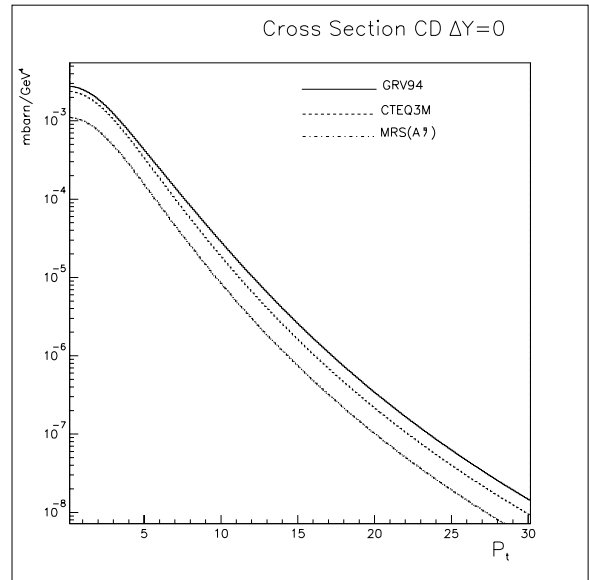


Fig.9b

Figure 9: (a) The cross section for $b\bar{b}$ diffractive production for the coherent diffraction (CD) (Eq. (29)) and the Ingelman - Schlein (IS) diffraction (Eq. (25)); (b) The cross section for $b\bar{b}$ for the coherent diffraction (CD) in different parameterizations for the gluon structure function.

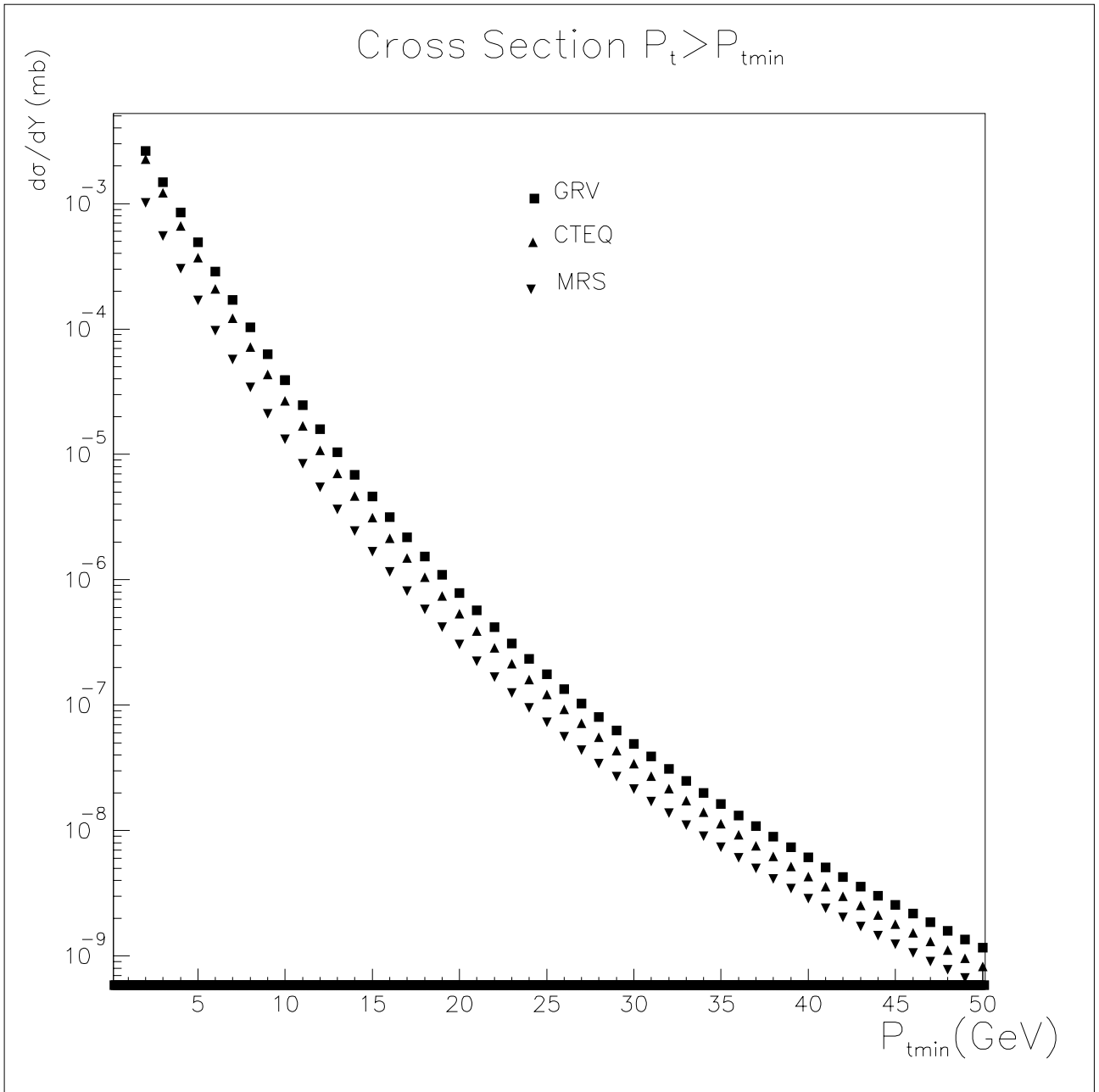


Figure 10: The integrated cross section for the coherent diffraction (Eq.(32)) versus p_t^{min} in different parameterizations of the gluon structure function.